International Journal of Nanomedicine

Dovepress
Taylor & Francis Group

Open Access Full Text Article

ORIGINAL RESEARCH

Combined Docetaxel-Loaded Perfluorocarbon Nanodroplets with Ultrasound-Mediated Blood–Brain Barrier Disruption for Effective Glioblastoma Treatment in Mice Model

Charlotte Bérard[1,*], Stéphane Desgranges[2,*], Noé Dumas[3], Anthony Novell[4], Erwan Selingue[5], Mourad Hamimed[6], Olivier P Chevallier[7], Charles Truillet[4], Benoit Larrat[5], Nicolas Taulier[8], Florian Correard[1], Christiane Contino-Pépin[2,*], Marie-Anne Estève[1,*]

[1]Aix Marseille Univ, APHM, CNRS, INP, Inst Neurophysiopathol, Hôpital Timone, Service Pharmacie, Marseille, France; [2]Avignon Université, SAFE, UPRI, Avignon, France; [3]Aix Marseille Univ, CNRS, INP, Inst Neurophysiopathol, Marseille, France; [4]Université Paris-Saclay, CEA, CNRS, INSERM, BioMaps, SHFJ, Orsay, France; [5]Université Paris-Saclay, CEA, CNRS, BAOBAB, Neurospin, Gif-sur-Yvette, France; [6]Aix Marseille Univ, CNRS, INSERM, Institut Paoli-Calmettes, CRCM, SMARTc Unit, COMPA Inria – Inserm project team, Marseille, France; [7]Avignon Université, Plateforme 3A, Avignon, France; [8]Sorbonne Université, CNRS, INSERM, Laboratoire d'Imagerie Biomédicale, LIB, Paris, F-75006, France

*These authors contributed equally to this work

Correspondence: Christiane Contino-Pépin, Avignon Université, SAFE, UPRI, Avignon, France, Email christine.pepin@univ-avignon.fr; Marie-Anne Estève, Aix Marseille Univ, APHM, CNRS, INP, Inst Neurophysiopathol, Hôpital Timone, Service Pharmacie, Marseille, France, Email marie-anne.esteve@univ-amu.fr

Introduction: Glioblastoma (GBM) remains the most aggressive primary brain tumor, characterized by a high recurrence rate and a poor prognosis, particularly due to the blood-brain/tumor barrier, which severely limits the intracerebral drug delivery. This study evaluates a novel strategy combining a nanomedicine-based drug delivery approach with focused ultrasound-mediated blood–brain barrier disruption (FUS-BBBD) to achieve localized therapeutic drug concentrations to the tumor.

Methods: Paclitaxel and docetaxel were encapsulated in perfluorooctyl bromide nanodroplets, stabilized with fluorinated surfactants. The formulation was optimized and characterized in terms of drug loading, encapsulation efficiency, size, size distribution and stability. In vivo pharmacokinetics (PK) and safety were assessed in C57BL/6 mice. Therapeutic efficacy was evaluated using an orthotopic syngeneic GL261 glioma model combined with hemispheric 1.5 MHz FUS-BBBD.

Results: Docetaxel-loaded nanodroplets (DTX-NDs) emerge as the most promising candidates. Optimized DTX-NDs exhibited a mean diameter of 62 ± 4 nm with an encapsulation efficiency exceeding 90%, a good stability achieved by freeze-drying, and a sustained release profile. PK analysis demonstrated a 28-fold reduction in systemic clearance and a significantly prolonged terminal half-life compared to free docetaxel. Quantitative LC-MS confirmed that FUS-BBBD enhanced docetaxel accumulation 9-fold in healthy brain tissue ($p < 0.05$) and 6-fold in GL261 glioma-bearing mice ($p < 0.05$) when using the nanodroplet formulation. An optimized treatment plan with DTX-NDs (20 mg kg^{-1} every 72 hours) successfully balanced efficacy and safety, extending median survival to 36 days versus 20 days for free DTX ($p < 0.05$), while achieving a 33% long-term survival rate. Toxicity was limited to transient and reversible hepatotoxicity.

Conclusion: This study demonstrates that the repeated combination of DTX-NDs and FUS-BBBD is a biocompatible and effective strategy for enhancing brain drug delivery while minimizing peripheral toxicity, thereby offering a promising translational approach for the treatment of GBM.

Keywords: brain tumor, nanoemulsions, drug delivery, focused ultrasound-mediated blood–brain barrier disruption

Introduction

Among gliomas, glioblastoma (GBM) is the most common and aggressive primary malignant brain tumor, accounting for approximately 48% of all primary malignant brain and central nervous system tumors in adults with an average annual incidence of 3 per 100 000 people in developed countries.[1] GBM is highly infiltrative and is characterized by high recurrence

https://doi.org/10.2147/IJN.S571560
Received: 4 November 2025
Accepted: 2 February 2026
Published: 11 April 2026

Graphical Abstract

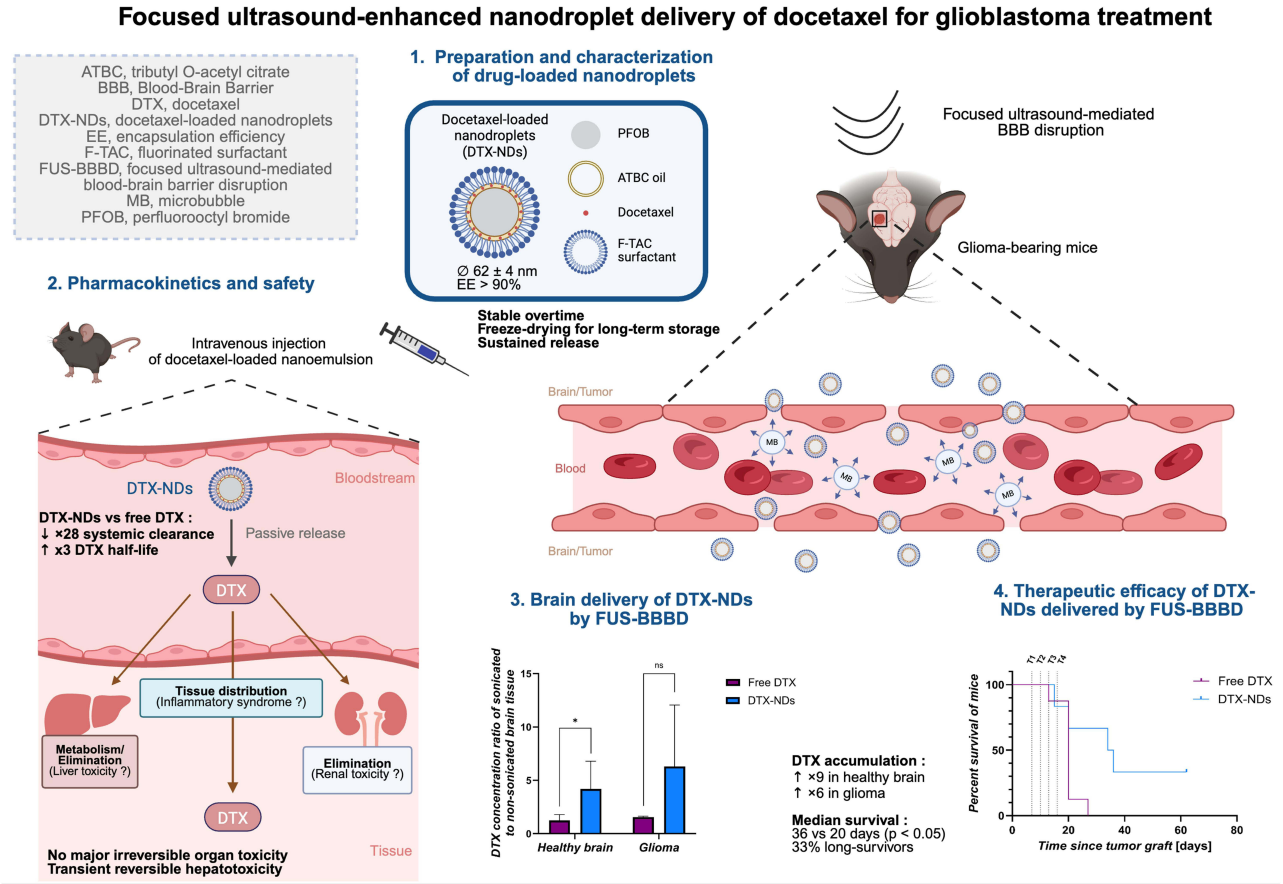

and very poor prognosis. Despite important advances in its understanding and many therapeutic innovations over the last few decades, GBM remains incurable and one of the deadliest cancers, with a 5-year survival rate following diagnosis below 10%.[2,3] Although the standard of care (combining maximal surgical resection and adjuvant radio-chemotherapy) increases the median survival from less than 4 months to 15 months in patients receiving treatment,[4] recurrence is still observed in 75% to 90% of patients within six months after treatment.[5] Multiple constraints make therapeutic innovation complex in GBM. Among them, the blood–brain barrier (BBB) represents a major issue to deliver anticancer drugs at effective concentration in the brain tumor tissue. As the tumor progresses, its vasculature becomes increasingly heterogeneous and the cerebral vessels display a tortuous architecture with a partially disrupted BBB, so-called the blood-tumor barrier (BTB). Although the integrity of the BBB is partially compromised in the presence of GBM, the BTB exhibits markedly heterogeneous permeability. Furthermore, tumoral regions with an intact BBB composed of many efflux transporters persist, which (i) are not visible on contrast-enhanced magnetic resonance imaging (MRI), (ii) have been identified as the preferential anatomical sites of recurrence, and (iii) prevent the delivery of anticancer agents.[6–8] Thus, there is a clear need for therapeutic and/or technical innovations capable of achieving sufficient and homogenous delivery of anticancer therapies at the brain tumor site to improve patient outcomes.

Many invasive or non-invasive strategies have been developed to overcome the BBB issues and enhance intracerebral drug delivery.[9–11] Among non-invasive approaches, biocompatible nanoparticles have been developed as drug carriers (eg, nanocarriers (NCs)) to exploit the advantages of nanoplatforms. These include improving the solubility of the drug, protecting it from degradation, prolonging its circulatory half-life and enabling passive targeting of tumors through the "enhanced permeability and retention" effect and active targeting through functionalization.[12] NCs can also reduce

toxicity in healthy tissue and enable controlled release. Although they have the potential to improve drug delivery into the brain, the limited number of translational successes impose combining the NC approach with an additional precise intracerebral delivery strategy to achieve an efficient drug concentration into the tumor.[9]

Among them, the use of transcranial pulsed ultrasound combined with gas-filled microbubbles (MBs) provides a physical method for non-invasive, local, and reversible BBB disruption. This technique, called focused ultrasound-mediated BBB disruption (FUS-BBBD), has been shown to be safe in both small and large animal models,[13] even with repeated BBB disruption.[14,15] Improvement of therapeutic outcomes has been achieved in several preclinical studies combining FUS-BBBD with a range of anticancer drugs or various drug formulations (drug-loaded MBs or drug-loaded NCs) in different preclinical glioma models.[16–18] Also, multiple clinical trials have been initiated within the last decade in patients with newly diagnosed or recurrent GBM.[18]

In our previous work, we have developed a novel formulation consisting of perfluorooctyl bromide (PFOB) nanodroplets (NDs) stabilized with fluorinated surfactants (called F-TACs) as safe NCs for the delivery of hydrophobic drugs into the brain after FUS-BBBD.[19] These nanoemulsions exhibit several properties that are fundamental to their use in GBM treatment including optimal nano-size for crossing the disrupted BBB, the ability to encapsulate hydrophobic drugs, stability during freeze-drying process for long-term storage. They are also internalized in cells through a rapid, time-dependent and non-saturable uptake, localizing mainly in the cytoplasm without nuclear penetration. GBM cells also exhibit faster and more extensive internalization than non-cancerous cells. In vivo, they have shown biocompatibility and tolerability following intravenous (i.v.) injection, long circulation time with no apparent toxicity in healthy mice, and safe brain delivery after FUS-BBBD.

For the present study, paclitaxel (PTX) and docetaxel (DTX) were chosen to be encapsulated into the droplet core. PTX and DTX are hydrophobic chemotherapeutic agents belonging to the taxanes class. They are clinically effective against a wide range of cancers but they do not penetrate the BBB. Among them, DTX appeared to be the best candidate for encapsulation in our NDs due to its higher solubility in their inner oily core. Various DTX-loaded nanoplatforms have already demonstrated an enhanced therapeutic efficacy in preclinical glioma models compared to branded formulations of DTX (ie, Taxotere®).[20–22] However, to our knowledge, no study evaluating DTX-loaded NCs combined with FUS-BBBD in GBM has been reported.

Herein, DTX-loaded NDs (DTX-NDs) have been assessed as a suitable effective formulation in combination with FUS-BBBD for the treatment of GBM. First, we studied the pharmacokinetic (PK) behavior of our formulation, and its preclinical safety compared to a branded formulation of DTX (Docetaxel Accord® 20 mg mL^{-1}). Then, the enhanced DTX accumulation in brain was investigated in healthy and glioma-bearing mice after a single or repeated administration of DTX-NDs combined with the FUS-BBBD procedure, in comparison to free DTX. Finally, improvement in therapeutic outcomes was evaluated in glioma-bearing mice while determining the optimal treatment plan with the best efficacy/tolerability ratio.

Materials and Methods

For Materials, see Supplementary data, section 1 in Materials and methods.

Preparation and Characterization of Drug-Loaded Nanodroplets

Oil Preparation

In a 2 mL vial, PTX was added in excess to each Capryol® 90 (C-90) and tributyl O-acetyl citrate (ATBC) oil, then the resulting suspension was stirred with a magnetic stirrer for at least 48 hours at room temperature. The vial was centrifuged at 5,580 *g* for 10 minutes, and the supernatant was titrated by high performance liquid chromatography (HPLC) after 400-fold dilution of the sample with acetonitrile (ACN). The oil was kept at 4 °C until further use. The same procedure was applied for DTX in C-90 and ATBC, but the suspension stirring time was limited to 3 hours as no significant improvement in drug solubilization was observed beyond this time.

Emulsion Preparation

A 50 mL centrifuge tube was filled with an oil solution (ATBC or C-90) loaded with either PTX or DTX followed by addition of PFOB. Then, 2 mL of surfactant solution (variable amounts of F_8TAC_{13} in 2 mL of water) were added. The

general composition of the different emulsion types (E1 to E5), containing either PTX or DTX dissolved in ATBC or C-90 oil, is described in Table 1. The mixture was cooled to 0 °C with an ice bath and insonified in pulsed mode (PM) (duty cycle (DC) 11.97%, pulse width of 8 s) with a sonicator (VibraCell. TM. 75043, 750 W, Bioblock Scientific, USA), using a 13 mm sonotrode, situated at the bottom of the centrifuge tube, at 60% amplitude. The total sonication duration was 2 minutes. The emulsion was centrifuged at 5,580 *g* for 5 minutes, the supernatant was then filtered through a 0.22 µm CA filter before size measurement by Dynamic Light Scattering (DLS) and titration of the drug content by HPLC. Six 300 µL aliquots of the emulsion were prepared and subsequently freeze-dried; drug titration and size measurement were re-evaluated after rehydration of one aliquot from each prepared batch (Table 1).

Freeze-Drying Process

Three hundred microliters of emulsion were introduced in a 2 mL vial and completed with 90 µL of an aqueous solution of trehalose ([trehalose] = 357 mg mL^{-1}) giving rise to a final trehalose concentration of 10.7% *w/v* after rehydration. Each vial was vortexed for 10 seconds. After being frozen at −20 °C for at least 2 hours, the vials were freeze-dried for 16 hours. Vials were stored at 4 °C until use. Before use, each vial was reconstituted by adding the lost water (240 µL).

Drug Loading and Encapsulation Efficiency Quantification by HPLC

HPLC analyses were conducted on an Alliance Waters system (e2695) equipped with a 2998 photodiode array detector (Saint-Quentin, France). Titration was carried out using a Sunfire C18 column from Waters (4.6 × 150 mm, 3.5 µm). A linear gradient of water and ACN ranging from 10% to 80% over 20 minutes was applied. The detection wavelength for the titration of PTX and DTX was 227 nm. The drug loading (DL) of the whole emulsion ([Drug]whole) was determined by HPLC following a twofold dilution with water. To assess the encapsulation efficiency (EE), each emulsion sample was centrifuged at 25,830 *g* for 45 minutes. The drug content in the supernatant ([Drug]sup), ie, free drug or drug encapsulated in micelles, was titrated by HPLC. EE was determined as follows: EE in % = (([Drug]whole-[Drug]sup) / [Drug]whole) × 100.

Determination of Nanodroplet Size

The nanodroplet size and size distribution were measured using a DLS apparatus (Zeta Sizer Nano-S, Malvern Instruments, Orsay, France) as previously described.[19] Hydrodynamic diameter (D_H) and polydispersity index (Pdi) are averages of 6 measurements and reported as an intensity-based distribution using the cumulant method (Z-average).

Transmission Electron Microscopy Images

Transmission Electron Microscopy (TEM) observations were conducted using a TEM Hitachi 7800–120 kV instrument as previously described.[19]

Determination of Docetaxel Release Profile

Previously prepared and freeze-dried emulsions were reconstituted in a 2 mL vial by adding 240 µL of water to each powder aliquot (to give a final volume of 300 µL) and then diluted with 1.7 mL of Phosphate Buffer Saline (PBS) solution. Given that one batch of emulsion provides at least six powder aliquots, one aliquot from the same batch was

Table 1 General Composition of the Different Emulsion Types

Emulsion	E1	E2	E3	E4	E5
Fv[a)]	4.7%	16.7%	26.0%	16.7%	16.9%
PFOB	95 µL	380 µL	665 µL	380 µL	380 µL
Oil[b)]	5 µL	20 µL	35 µL	20 µL	27 µL
F_8TAC_{13}	50 mg	200 mg	266 mg	155 mg	155 mg
Water	2 mL	2 mL	2 mL	2 mL	2 mL
Sur[c)]	25.0 mg mL^{-1}	100.0 mg mL^{-1}	133.0 mg mL^{-1}	77.5 mg mL^{-1}	77.5 mg mL-1^{-1}

Notes: [a)]Fv= Volume fraction of the dispersed phase; [b)]Drug-loaded oil solution; [c)]*Sur*= Concentration of surfactant F_8TAC_{13} expressed in mg mL^{-1} of water. The dispersed phase is made of 95% of PFOB and 5% of oil for samples E1 to E4 and of 93% of PFOB and 7% of oil for sample E5.

used for each time point in each separate experiment. Reconstituted samples were kept at 37 °C under magnetic stirring for either 0, 1, 2, 4 or 8 hours. At each time point, the sample was centrifuged at 4 °C for 1 hour at 25,830 *g* to allow the droplets to settle. Then, the supernatant was collected (800 µL) and titrated by HPLC. The DTX concentration in the supernatant ([DTX]sup) at T0 was subtracted from the titration of the other time points and then plotted as percentage of cumulative release. The 100% was defined as the titration of the [DTX] of the whole emulsion ([DTX]whole) at T0 minus the [DTX]sup at T0. Experiments were performed in triplicate.

In vitro Evaluation of Anticancer Activity of ATBC/Docetaxel and C-90/Docetaxel Oil Phases

Human GBM cell line (U87-MG) was obtained from American Type Culture Collection (ATCC) and was cultured as previously described.[19] To evaluate the anticancer activity of the ATBC/DTX and C-90/DTX oil phases, U87-MG cells were seeded on 96-well plates (12,500 cells cm^{-2}) and allowed to grow for 24 hours prior to treatment. Then, cells were treated for 72 hours with a range of DTX concentrations (0.1, 1, 2.5, 5, 10, 50 nmol L^{-1}) dissolved in DMSO, ATBC or C-90, and dispersed in culture medium. Cell viability was assessed by using a colorimetric assay with 3-(4,5-dimethylthiazol-2-yl)-2,5-diphenyltetrazolium bromide (MTT) as previously described.[23] Viability was calculated as measurement of absorbance from a sample, normalized to the absorbance from control cells.

In vivo Studies Using the Animal Model

All in vivo experiments were performed using 6-week-old (16–18 g) female C57BL/6 mice (Envigo, Indianapolis, USA) after a seven-day acclimatization period to the laboratory conditions. All animal procedures were carried out in conformity with the guidelines of the French Government and the Regional Committee for Ethics on Animals Experiments for the care and use of laboratory animals (CE71, Aix Marseille Université, project reference: APAFIS#26725-2020052816206649, laboratory accreditation number: A1305532). For each in vivo experiment requiring anesthesia, mice were anesthetized with an intraperitoneal injection of ketamine/xylazine (100 mg kg^{-1} and 10 mg kg^{-1}, respectively, 0.1 mL per 10 g of weight). Free DTX or DTX-NDs or NaCl 0.9% or SonoVue® (Bracco Imaging, Italy) was administered by retro-orbital i.v. injection using an 8 mm 30-gauge needle attached to a 0.5 mL insulin syringe (BD Micro-Fine™, Becton, Dickinson and Co., Franklin Lakes, NJ, USA). Euthanasia was performed at the end of the procedure or when the animal showed signs of suffering (eg, suffocation, a prone posture, bristly fur, weight loss exceeding 20% of maximum weight). For all procedures requiring blood sampling, animals were anesthetized prior to blood collection by intracardiac puncture and sacrificed. All mice were sacrificed by cervical dislocation.

Determination of Pharmacokinetic Parameters Using in vivo Model

Ninety healthy mice were divided into two experimental groups and received a single equivalent dose of 20 mg kg^{-1} of free DTX or DTX-NDs. In each group, mice were divided into 9 subgroups (5 mice per subgroup) corresponding to 9 sampling time-points (5, 10, 30, 60 minutes and 2, 4, 16, 24 and 48 hours). At pre-determined time points, mice were anesthetized and sacrificed for blood collection. The whole blood was collected into heparin coated tubes by intracardiac puncture. Blood samples were stored at −80 °C until samples extraction for determination of DTX content by Liquid Chromatography-Mass Spectrometry (LC-MS). The DTX concentration–time profile curves were obtained by averaging the dosage values of 5 mice per sampling time. Naïve-pooled concentration–time data (ie, assuming that the data were obtained from a single mouse) were evaluated using a non-compartmental analysis approach. The PK parameters as well as systemic exposure measures, including observed concentration at the 5th minute after the end of i.v. injection (C_{max}), area under the plasma concentration–time curve (AUC), terminal half-life ($t_{1/2}$), total clearance (Cl), and volume of distribution (V_d) were estimated using PKanalix software, version 2021R1 (Antony, France: Lixoft SAS).

In vivo Toxicity Studies Using Determination of Biochemical Parameters

Thirty healthy mice were divided into two experimental groups (15 mice per group) and a single equivalent dose of 20 mg kg^{-1} of free DTX or DTX-NDs was intravenously administered. In each group, mice were divided into 3

subgroups (5 mice per subgroup) corresponding to 3 selected time points for blood sampling (1, 7 and 14 days). At predetermined time points, mice were anesthetized and sacrificed for blood collection. The whole blood was collected into heparin coated tubes by cardiac puncture and centrifuged at 400 *g* for 10 minutes. The plasma was collected and stored at –80 °C until determination of biochemical parameters of liver function (Alanine aminotransferase (ALAT), Aspartate aminotransferase (ASAT)), kidney function (creatinine) and an inflammatory marker (interleukin-6, IL-6). The metabolic exploration was performed by Phenomin-ICS (Institut Clinique de la Souris, Illkirch, France). Mice body weight and behavior were monitored after DTX or DTX-ND administration to explore the presence of toxic effects.

Focused Ultrasound-Mediated Hemispheric Blood-Brain Barrier Disruption Procedure

Hemispheric BBB permeabilization (6 mm × 3.6 mm × 5 mm) was achieved using a focused transducer mounted on a 3D motor allowing continuous raster scan at 10 mm/s (central frequency at 1.5 MHz, active diameter 25 mm, focal depth 20 mm, width of focal spot at −6 dB 1 mm, length of focal spot at −6 dB 5 mm, Imasonic, France) connected to a single-channel programmable generator (Image Guided Therapy, Pessac, France). A bolus (60 µL) of commercially available MBs (SonoVue®) was administered immediately before starting transcranial sonication (FUS) above the right hemisphere in anesthetized animals. The experimental FUS-BBBD procedure was the same as previously described.[19,24]

Quantitative Analysis of Docetaxel Accumulation in Healthy Mice Brain Following Focused Ultrasound Exposure

Eight healthy mice were divided into 2 treatment groups and intravenously administered free DTX (n = 4) or DTX-NDs (n = 4) at an equivalent dose of 20 mg kg^{-1} of DTX, ten minutes before FUS-BBBD hemispheric procedure. The left hemisphere was not sonicated and was used as control. Mice were sacrificed 1 hour post BBB permeabilization and perfused with saline through the left ventricle. Brains were collected immediately, and the sonicated hemisphere was separated from the contralateral non-sonicated hemisphere. Half brain samples were stored at −80 °C until samples extraction for determination of DTX content by LC-MS as described in Determination of Docetaxel in Blood and Brain Tissue Using LC-MS Analysis.

GL261 Glioma Tumor Model

To quantify the accumulation of DTX or DTX-NDs in brain tumor and to evaluate their therapeutic efficacy, GL261 glioma-bearing C57BL/6 mice, an orthotopic syngeneic murine glioma model, were prepared. Mice were anesthetized and placed on a stereotactic frame (Kopf instruments, CA, USA). A skin incision was made on the scalp and a burr hole was drilled into the skull of the right hemisphere. Mice received a 2 µL injection of Dulbecco's Phosphate-Buffered Saline (DPBS) containing 50,000 GL261 cells (from DSMZ, Germany, cultured in Dulbecco's Modified Eagle Medium (DMEM) with 10% fetal calf serum (FCS) and 1% (v/v) of penicillin/streptomycin) into the right striatum (2 mm lateral and 1 mm anterior from the bregma and 3 mm depth from bone). After positioning of the needle (Hamilton 702 N) with the stereotactic frame, injection was performed using a syringe pump (Kd Scientific, Legato® 130 Syringe Pump, MA, USA) at a rate of 0.5 µL min^{-1} over 4 minutes. The needle was kept in place for 5 minutes before its retraction at a rate of 0.5 mm min^{-1}. The wound was then closed with tissue adhesive glue (3M Vetbond®, Cergy-Pontoise, France) or a suture. These glioma-bearing mice were raised under standard conditions for one week before being used for subsequent experiments.

Experimental Design and Treatment Plans of the in vivo Efficacy Studies

A total of 61 glioma-bearing C57BL/6 mice were used to evaluate therapeutic efficacy. Mice were divided into 4 experimental groups.

In all experimental groups, the FUS-BBBD hemispheric procedure was performed on the hemisphere bearing the tumor ten minutes after each i.v. administration of NaCl 0.9%, free DTX, or DTX-NDs.

In the first experimental group, the amount of DTX delivered to the brain tumor by FUS-BBBD was investigated. Five glioma-bearing mice received free DTX (n = 2) or DTX-NDs (n = 3) at an equivalent DTX dose of 20 mg kg^{-1} on

days 7, 9 and 11 after tumor graft. Brain hemispheres were collected 11 days post-graft as described above and stored at –80 °C until samples extraction and determination of DTX content by LC-MS.

In the second experimental group, 24 mice were divided into 3 subgroups in order to evaluate the efficacy of a first therapeutic protocol: the control subgroup (treated with NaCl 0.9%, n = 10), the group treated with free DTX (n = 6), and the group treated with DTX-NDs (n = 8). A total of four treatments were administered on days 7, 9, 14 and 16 after tumor graft (2 sessions of 2 administrations 48 hours apart, of NaCl 0.9%, DTX or DTX-NDs, equivalent DTX dose of 20 mg kg^{-1}).

The third and fourth experimental groups aimed at optimizing the therapeutic plan (ie, improve the efficacy/tolerability ratio).

The third experimental group divided 18 mice into 2 subgroups: treatment with free DTX (n = 9) or DTX-NDs (n = 9). A total of four treatments were administered on days 7, 10, 13 and 16 after the tumor cell graft (4 administrations of DTX or DTX-NDs, with an initial dose equivalent to 20 mg kg^{-1} of DTX and subsequent doses equivalent to 10 mg kg^{-1} of DTX, at 72-hour intervals).

The fourth experimental group divided 14 mice into 2 subgroups: treatment with free DTX (n = 8) or DTX-NDs (n = 6). A total of four treatments were administered on days 7, 10, 13 and 16 after the tumor cell graft (4 administrations of DTX or DTX-NDs, with an equivalent DTX dose of 20 mg kg^{-1}, at 72-hour intervals).

For the experimental groups 2, 3 and 4, therapeutic outcomes were investigated through monitoring the survival time and weight of each mouse. Mice were sacrificed if they experienced a weight loss exceeding 20% of their maximum weight or presented any signs of distress (eg, suffocation, a prone posture, bristly fur).

Determination of Docetaxel in Blood and Brain Tissue Using LC-MS Analysis

PTX was added as an internal standard (IS) and mixed briefly with each blood and brain halves tissue samples (300 ng for PK studies, 20 ng for the brain delivery of DTX-NDs after FUS-BBBD in healthy mice study or 30 ng for the brain delivery of DTX-NDs after repeated FUS-BBBD in glioma-bearing mice study). Brain halves samples were then homogenized in DPBS (300 µL) using a T25 Ultra-Turrax® (IKA, Staufen, Germany). Tissue homogenizer was rinsed twice with 300 µL of DPBS and fractions were pooled. Blood or brain samples were extracted 3 or 4 times, respectively, with methyl tert-butyl ether (MTBE) (500 µL) and vortexed. Supernatants were separated after centrifuging at 21,500 *g* for 5 min, collected in Eppendorf tubes and evaporated in 60 °C water bath for 2 hours. Dried extracts were stored at −80 °C until further analysis.

Blood sample preparation protocol prior LC-MS injection: each dry sample was reconstituted with 1 mL of a solution consisting of a 60:40 mixture of ACN and water, the sample was then vortexed and homogenized with the help of an ultrasound bath for 15 minutes. Ten µL of this solution were diluted with 990 µL of the previous solvent mixture and subsequently filtered over 0.22 µm PTFE, then diluted 20 times directly in HPLC vial (20 µL diluted with 380 µL of solvent mixture).

Brain samples preparation protocol prior LC-MS injection: each dry sample was reconstituted with 100 µL of diethyl ether (Et_2O) and vortexed, then 200 µL of methanol was added and Et_2O was evaporated at 40 °C for 30 minutes. The samples were then centrifuged for 5 minutes at 25,830 *g* and the supernatants were evaporated using miVac duo centrifugal concentrator (Genevac®, SP Scientific Products, UK) for 2 hours. Finally, 200 µL of methanol were added and filtered over 0.22 µm PTFE centrifuge filter.

Standard curves were established by spiking DTX in respective matrices (blood or brain tissue) to yield final amounts of DTX between 0.0192 and 300 µg for PK studies, DTX-NDs between 0.2 and 100 ng for the brain delivery of DTX-NDs after FUS-BBBD in healthy mice study, and between 0.41 and 33.33 ng for the brain delivery of DTX-NDs after repeated FUS-BBBD in glioma-bearing mice study, then they were processed in the same way as the samples.

DTX quantification was performed with an Acquity I-Class UPLC system (Waters, Milford, MA, USA) hyphenated to a mass spectrometer Xevo TQ-XS (Waters, Milford, MA, USA) equipped with an electrospray ionization source. The MS was operated in Multiple Reaction Monitoring mode (for details, see Supplementary data, section 2 in Materials and methods). The expected retention times for DTX and IS were 2.77 and 2.85 minutes, respectively. No significant interferences from endogenous substances were observed at the retention times of the analyte and IS. Also, studies showed that there were no endogenous interferences in blank tissues. Peak ratios of DTX to PTX were plotted against nominal concentration of DTX to generate a calibration curve from blood and brain tissue.

 https://doi.org/10.2147/IJN.S571560

Magnetic Resonance Imaging

MRI was used to confirm the presence of brain tumors before the therapeutic protocol. Briefly, T1-weighted contrast-enhanced MRI images were acquired with a 7T/90mm bore hole MRI scanner (Pharmascan scanner, Bruker, Germany). A Gadolinium-based contrast agent (Dotarem®, Guerbet, France) was intravenously injected (100 µL by animal) via a catheter. T1-weighted images were then acquired (MSME sequence, TE/TR = 8/340 ms, 10 averages, matrix = 256 × 256 × 64, resolution = 0.15 × 0.15 × 0.60 mm^3, 10 averages, acquisition time = 6 min).

Statistical Analysis

All the data were presented as mean ± standard deviation. Statistical analysis was performed with GraphPad Prism 10.4.2 (La Jolla, CA, USA). The comparison of DTX brain delivery after FUS-BBBD in healthy mice or glioma-bearing mice between free DTX and DTX-NDs groups used unpaired Student's *t*-test. The survival time of the different treatment groups was recorded from the day of tumor graft until death. The Kaplan–Meier method was used to plot animal survival curves. The median survival time, maximal survival time and the increase in median survival time (IST_{median}) were compared. Significance was assessed by using the Mantel-Cox Log Rank test. A p-value less than 0.05 was considered statistically significant.

Results

Preparation and Characterization of Drug-Loaded Nanoemulsions

In a previous publication, NDs with a mean diameter around 50 nm, capable to deliver hydrophobic compounds to the brain after FUS-BBBD were developed.[19] The surface of these NDs was stabilized by an in-house surfactant called F_8TAC_{13}, while their core was made of PFOB and a biocompatible oil (ATBC or C-90), the latter oily phase enabling a drug or a dye to be encapsulated into the droplets. Various [oil/dispersed phase] ratios were studied in order to balance the droplet size, size distribution (as small and monodisperse as possible) and oil volume (for improved drug encapsulation). The best trade-off was achieved using 5% ATBC and 10% C-90, giving rise to droplets of 47 and 51 nm diameter, respectively. In both cases, the volume fraction (Fv) of NDs in the resulting emulsions, corresponding to the volume of the dispersed phase ($\Phi_{dispersed}$=PFOB + oil) within the whole emulsion, was 4.7%. These emulsions were freeze-dried in 300 µL aliquots which could be resuspended in smaller (ie, concentrated), equal or larger (ie, diluted) volumes of water without altering the droplet size.

These previous results were used as starting conditions for the preparation of drug-loaded NDs in the current study. Optimization experiments were first carried out on PTX before being transposed to DTX.

Preparation of a Paclitaxel-Saturated Dispersed Phase

In order to achieve a drug dose of 20 mg kg^{-1} for in vivo assays, equivalent to 0.32–0.36 mg per mouse of approximately 16–18 g body weight, the intended optimal drug concentration (PTX) for emulsions is 1.07–1.2 mg mL^{-1}, for aliquots of 300 µL before freeze-drying. To achieve this dose, two oil solutions (ATBC and C-90) saturated with PTX were prepared. Their drug concentrations, determined by HPLC, were 18 mg mL^{-1} and 49 mg mL^{-1} for ATBC and C-90, respectively (Figure 1a). The most concentrated solution, ie, the C-90/PTX oily phase, was then used to optimize the DL of the emulsion.

Optimization of Drug Loading and Encapsulation Efficiency for Paclitaxel-Loaded Nanodroplets

DL and EE were considered along with droplet size to optimize the encapsulation of PTX. DL represents the amount of drug in the total emulsion (referred as [Drug]whole), while EE is the percentage of drug encapsulated in NDs as previously expressed (see Drug Loading and Encapsulation Efficiency Quantification by HPLC in Materials and Methods). It appeared that in order to preserve the same range of ND size, the [oil/dispersed phase] ratio had to be adjusted when a drug was dissolved into the oily phase. For the C-90/PTX oily phase, this ratio fell to 5% against 10% for the pure C-90 oil (at 10% C-90/PTX, the ND size was above 500 nm) (data not shown).

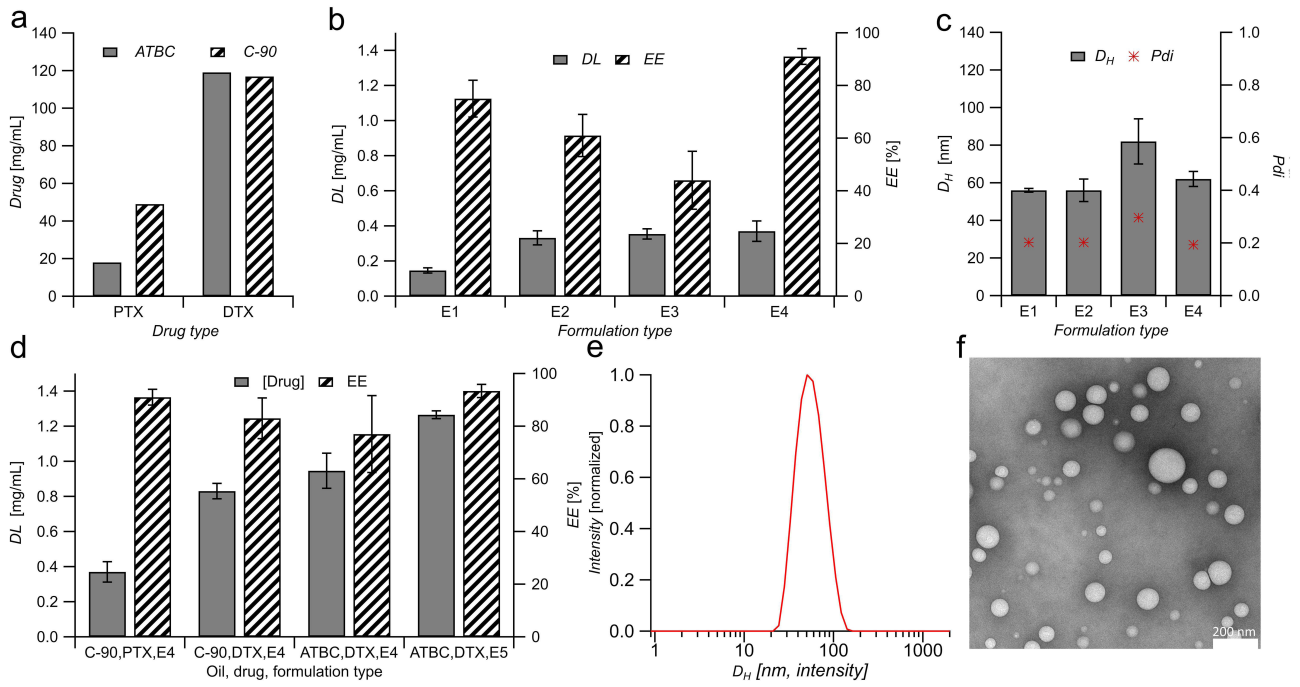

Figure 1 Characterization of drug-loaded nanoemulsions. (**a**) Concentration of PTX and DTX in ATBC and C-90 oils. (**b**) Drug loading (*DL*) and encapsulation efficiency (*EE*) of PTX-NDs emulsions (E1 to E4) of various volume fractions and surfactant concentrations (see Table 1). (**c**) Hydrodynamic diameter (D_H) and polydispersity index (Pdi) of NDs for emulsion samples E1 to E4. (**d**) *DL* and *EE* of PTX-NDs and DTX-NDs (emulsions E4 and E5) with C-90 or ATBC oil. (**e**) DLS spectrum of DTX-NDs (sample E5) after rehydration (cumulant analysis). (**f**) TEM image of DTX-NDs (sample E5) after rehydration.

Based on these data, an emulsion (E1, Table 1) with a Fv of 4.7% was first prepared, consisting of 95% of PFOB and 5% of C-90/PTX. The DL and EE were found to be 0.146 ± 0.015 mg mL^{-1} and 75 ± 7%, respectively, which was far from the intended concentration of 1.2 mg mL^{-1} for in vivo testing (Figure 1b).

Our strategy to achieve this desired DL was to increase the Fv of emulsions. To this end, two higher Fv were tested, namely 16.7% and 26.0% (E2 and E3, Table 1). As shown in Figure 1b, the DL reached a plateau at 16.7% of Fv and above, while EE evolved inversely to the Fv from 75 ± 7% for a Fv of 4.7% to 44 ± 11% for a Fv value of 26.0%. This could be due to the rise of surfactant concentration (*Sur*) in the aqueous solution, from 25.0 mg mL^{-1} to 133.0 mg mL^{-1} for Fv values of 4.7% to 26.0%, resulting in an increase of PTX solubility in the water phase surrounding NDs (probably encapsulated in surfactant micelles). Moreover, at the higher Fv value (26%), the droplet size and Pdi increased (Figure 1c). Therefore, in order to maintain the maximum DL obtained for a Fv of 16.7%, while improving the EE, the surfactant concentration in the aqueous phase was reduced from 100.0 mg mL^{-1} (E2, Table 1) to 77.5 mg mL^{-1} (E4, Table 1). This resulted in an increase in EE from 61 ± 8% for E2 to 91 ± 3% for E4 (Figure 1b), with a ND diameter of 62 ± 4 nm and a narrow Pdi of 0.193 (Figure 1c). Despite this optimization in terms of EE, the DL value of 0.370 ± 0.058 mg mL^{-1} (Figure 1d) remained too low to consider in vivo testing of paclitaxel-loaded NDs (PTX-NDs), which led us to formulate another drug following the same approach.

Preparation of a Docetaxel-Saturated Dispersed Phase

DTX, which also belongs to the taxanes class of chemotherapeutics, was considered as an alternative to PTX. With a slightly higher LogP value than PTX (4.26 for DTX instead of 4 for PTX), DTX is reported to have a better solubility in C-90 than PTX.[25]

As was done for PTX, the solubility of DTX was screened into the two previously selected oils, ATBC and C-90, before the preparation of emulsions using both DTX-saturated oil solutions C-90/DTX and ATBC/DTX.

The DTX solubility was found to be 119 ± 7 mg mL^{-1} and 117 ± 16 mg mL^{-1} in ATBC and C-90, respectively (Figure 1a). Compared to the solubility of PTX in these two oils, it was more than 6-fold higher for ATBC and 2-fold higher for C-90. Although the solubility of DTX was similar in both oils, we observed that the C-90/DTX solution began

https://doi.org/10.2147/IJN.S571560

to precipitate after 24 hours, requiring the oil phase to be prepared just before the ND preparation. In contrast, the ATBC/DTX solution remained stable and could be stored at 4 °C for several days before use.

In vitro Anti-Glioma Activity of ATBC/Docetaxel and C-90/Docetaxel Oil Phase

To ensure that DTX retains its pharmacological activity when dissolved in ATBC or C-90 oil, survival of human GBM cell line (U87-MG) was measured and compared with that of DTX dissolved in DMSO. The IC50 (concentration at which cell survival is inhibited by 50%) of DTX remains identical whatever the vehicle: 3.3 ± 0.3 nmol L^{-1} in DMSO, 2.2 ± 0.2 nmol L^{-1} in ATBC and 4.3 ± 0.3 nmol L^{-1} in C-90 (Figure S1). The pharmacological activity of DTX is thus preserved in vitro. Both DTX-loaded oily phases were tested for the preparation of DTX-ND emulsions applying the same method as previously described for PTX-ND emulsions.

Optimization of Drug Loading and Encapsulation Efficiency for Docetaxel-Loaded Nanodroplets

The best condition obtained for PTX, ie, condition E4 of Table 1, was considered here for comparison purpose. As expected, the DL of C-90/DTX emulsions was twice that of C-90/PTX emulsions (0.83 ± 0.04 mg mL^{-1} for DTX vs. 0.37 ± 0.06 mg mL^{-1} for PTX). It was even better for DTX in ATBC oil, reaching a DL value of 0.95 ± 0.10 mg mL^{-1} (Figure 1d). For these formulations of DTX-NDs, EE were 83 ± 8% and 77 ± 15% for C-90/DTX and ATBC/DTX, respectively (Figure 1d). Based on these results and to the greater stability of the ATBC/DTX solution, we focused on DTX-NDs with ATBC oil for further optimization.

Although the DL was acceptable, the EE still needed improvement to maximize the concentration of DTX encapsulated into the core of NDs for future in vivo experiments (the intended optimal drug concentration is also 1.07–1.20 mg mL^{-1} for DTX emulsions, ie, 20 mg kg^{-1}). This was achieved by increasing the volume of the ATBC/DTX oily phase from 20 µL (E4, Table 1) to 27 µL (E5, Table 1), while keeping the volume of PFOB constant (380 µL). This resulted in a slight increase in the Fv of the emulsion to 16.9%. The surfactant concentration in the aqueous phase was maintained at the level previously optimized for PTX (ie, 77.5 mg mL^{-1}). This emulsion E5 exhibited a DL value of 1.27 ± 0.02 mg mL^{-1} and an EE value of 93 ± 2.5% (Figure 1d), for very small and monodisperse DTX-NDs (size (D_H) = 55 ± 2 nm; Pdi = 0.12 ± 0.02, Figure 1e). Overall, these results were in good agreement with the targeted DL (1.07–1.20 mg mL^{-1}) and ND size for BBB crossing in association with FUS-BBBD, as demonstrated in our previous work.[19] Therefore, we selected the DTX formulation E5 for in vivo experiments.

Freeze-Drying

To prevent an increase in the droplet size due to Ostwald ripening, a previously established freeze-drying process was applied.[19] The latter freeze-drying method, optimized for drug-free emulsions with an Fv of 4.7%, involved the use of trehalose as a cryoprotectant at a concentration of 5% (w/v). As shown in Table S1, this 5% trehalose concentration was not sufficient for DTX-loaded emulsions, resulting in a Sf/Si ratio of 1.36 (final size after rehydration of the freeze-dried emulsion (Sf)/initial size of the parent emulsion before freeze-drying (Si)). In order to improve this ratio, two other trehalose concentrations (10% and 15%) were tested. The best result was obtained with 10% of trehalose, yielding a Sf/Si ratio of 1.13. Therefore, this concentration of trehalose was chosen for the freeze-drying of all emulsion samples.

Nanodroplet Size and Dispersity Limits for in vivo Testing

To ensure reproducibility, acceptance of size and polydispersity for in vivo administration across batches, a series of emulsion batches was prepared for in vivo experiments. Each batch produced six freeze-dried aliquots, one of which was used for size and polydispersity control and DTX concentration ([DTX]) measurements. The other five were kept for in vivo experiments. After emulsion rehydration, the acceptable ND diameter threshold was set at 65 nm with a Pdi inferior to 0.2. A total of 57 emulsion batches were prepared (following conditions E5, Table 1) in order to perform all the biological assays. After rehydration of each control aliquot for the entire series, the resulting average diameter of NDs was 62 ± 4 nm, with an average Pdi of 0.17 ± 0.03, in good agreement with the fixed threshold for in vivo experiments. The ND size was also confirmed by TEM (Figure 1f) using ImageJ software. The average diameter was of 68 ± 26 nm. The smallest droplets had a diameter of 30 nm, whereas the largest had a diameter of 162 nm. A size distribution graph revealed that 92% of the droplets were less than 96

nm in diameter (Figure S2). Regardless of the method employed, the sizes fall within the same range: 62 nm by DLS and 68 nm by TEM. The average [DTX] was 1.13 ± 0.08 mg mL^{-1} of emulsion.

Emulsion Stability and Passive Release Follow-Up

The DTX release profile was assessed at 37 °C in a volume equivalent to the average blood volume of a mouse (approximately 2 mL). The release was monitored by HPLC for 8 hours, which is longer than the BBB half closure time for droplets around 60 nm in size after FUS-BBBD, according to the model by Marty *et* al[26,27] After 8 hours, approximately 40.2 ± 6.3% of the drug has been released from NDs, compared to 15.2 ± 5.7% after 1 hour. This suggests a sustained-release effect of DTX but no burst effect (Figure 2).

Thus, a stable formulation of DTX-NDs was developed. This emulsion meets the necessary criteria for ND size, dispersity, DL, EE and stability, making it suitable candidate for in vivo testing against GBM.

Pharmacokinetics and Toxicity Studies in Animal Model

To investigate the effects of DTX encapsulation on DTX PK, mice were injected with free DTX or DTX-NDs. The median DTX concentration–time curves in free DTX (Docetaxel Accord®) and DTX-NDs groups are shown in Figure 3a. The median concentration of DTX after 5 minutes (C_{max}) was significantly higher in the DTX-NDs group, reaching a C_{max} of 145.5 µg mL^{-1}, compared to 12.3 µg mL^{-1} for the free DTX group ($p < 0.01$). The blood concentrations of DTX were detected up to 2 hours for the commercial formulation, whereas drug levels remained detectable up to 4 hours for DTX-NDs, suggesting that DTX encapsulated in NDs would remain in the circulation for a longer time than free DTX. A non-compartmental analysis (a naive pooled data approach) was performed to extract PK parameters for both formulations, as reported in Table 2. A comparison of area under the curve $AUC_{0-\infty}$ showed that the ND formulation produced higher exposure levels (7,342 min µg mL^{-1} vs. 256 min µg mL^{-1}). Accordingly, total clearance of DTX-NDs was 28 times lower than that of free DTX (0.05 mL min^{-1} vs. 1.40 mL min^{-1}). DTX elimination half-life was prolonged from 21.5 minutes in free DTX group to 72.4 minutes in DTX-NDs group. The distribution of DTX was also significantly affected, with a volume of distribution (V_d) of 2.1 mL for DTX-NDs vs. 34.5 mL for free DTX. These results showed that the systemic exposure to DTX was significantly enhanced by the ND formulation through improvement in its PK properties. Therefore, it could be suggested that the surfactant shell of the NDs protects the drug and is responsible for the sustained-release effect of DTX.

To detect any potential signs of toxicity induced by DTX-NDs, healthy mice received a single dose either of free DTX (Docetaxel Accord®) or DTX-NDs at 20 mg kg^{-1} of DTX. All animals appeared healthy and exhibited normal activity, and no significant difference in body weights was noted up to 14 days after administration. Figure 3b–d, and e show the blood levels of biochemical parameters of liver function (ALAT, ASAT), kidney function (creatinine) and an inflammatory marker (IL-6), explored 1, 7 and 14 days after i.v. administration. One day after DTX-NDs injection, the median ALAT and ASAT levels were increased, approximately 5-fold (159 U L^{-1}) and 8-fold (410 U L^{-1}) above the upper limit

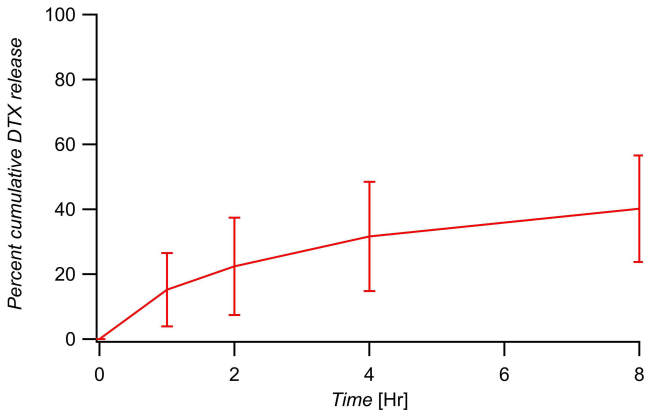

Figure 2 DTX release from NDs at 37 °C over time. The values are reported as mean ± SD (n = 3).

https://doi.org/10.2147/IJN.S571560

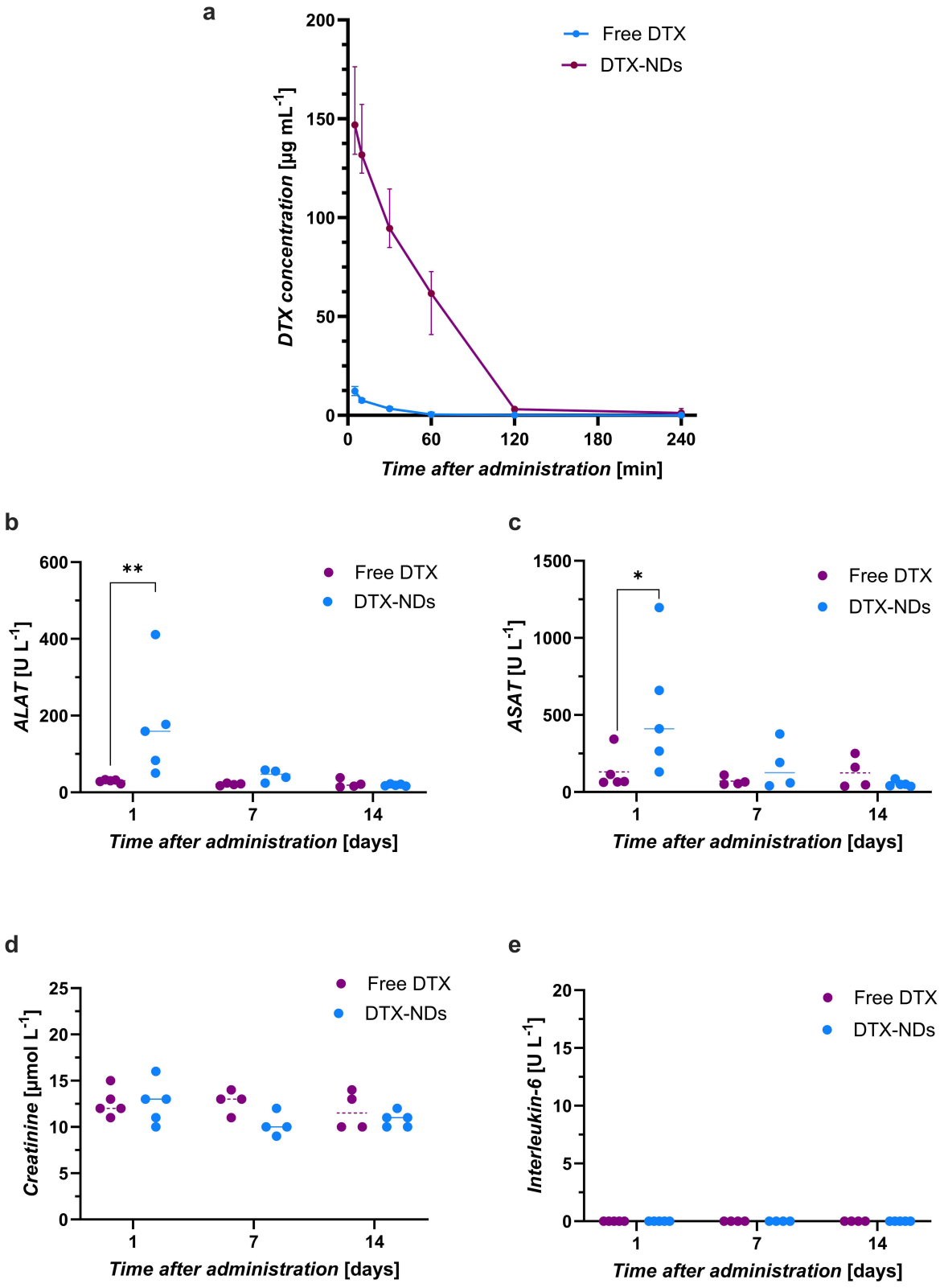

Figure 3 In vivo pharmacokinetics and safety comparison of free docetaxel (DTX) and docetaxel-loaded nanodroplets (DTX-NDs) in healthy mice. (**a**) Concentration-time profile of DTX in the bloodstream following a single intravenous administration of free DTX or DTX-NDs (intravenous injection, equivalent dose of 20 mg kg^{-1} of DTX). Data are expressed as median ± interquartile range (n = 5). Safety profiles of liver function (**b** and **c**), kidney function (**d**) and inflammation (**e**) 1, 7 and 14 days following a single intravenous dose of free DTX or DTX-NDs. Data are expressed as median (day 1: n = 5, day 7: n = 4, day 14: n = 4 for DTX group and n = 5 for DTX-NDs group). *p < 0.05, **p < 0.01, Student's *t*-test.

Table 2 Pharmacokinetic Parameters of Docetaxel (DTX), Using a Non-Compartmental Analysis, Following Intravenous Administration of a Single Dose of Free DTX or DTX-NDs (Equivalent Dose of 20 mg kg^{-1} of DTX)

Pharmacokinetic Parameters	Free DTX	DTX-NDs
$t_{1/2}$ (blood terminal half-life)	21.5 min	72.4 min
C_{max} (median maximum concentration)	12.3 μg mL^{-1}	145.5 μg mL^{-1}
V_d (volume of distribution)	34.5 mL	2.1 mL
Cl (clearance)	1.4 mL min^{-1}	0.05 mL min^{-1}
$AUC_{0-\infty}$ (area under the curve)	256 min μg mL^{-1}	7,342 min μg mL^{-1}

of normal (ULN), respectively, compared with those of the free DTX group which remained within normal values.[28] For DTX-NDs group, 7 days post-administration, the median ALAT and ASAT levels were only 1.5 and 2 times above the ULN, respectively.[28] Fourteen days post-administration, no elevated levels of serum transaminases were found, indicating transient signs of hepatotoxicity with the DTX-NDs formulation. Regardless of the administered formulation, creatinine levels remained within the normal range and IL-6 levels were undetectable on days 1, 7 and 14 post-administration, suggesting an absence of signs of renal toxicity or inflammatory syndrome.

Brain Delivery of Docetaxel-Loaded Nanodroplets After Focused Ultrasound-Mediated Blood-Brain Barrier Disruption in Healthy Mice

In our previous work,[19] we showed that i.v. injection of NDs in combination with FUS-BBBD using SonoVue® MBs has the potential to achieve non-invasive, safe, and localized drug delivery into the brain. We therefore assessed whether the DTX-NDs formulation combined with hemispheric FUS-BBBD increased DTX penetration into the brain (see treatment plan in Quantitative Analysis of Docetaxel Accumulation in Healthy Mice Brain Following Focused Ultrasound Exposure in Materials and Methods). Figure 4a shows the DTX concentrations per unit mass in sonicated and contralateral non-sonicated brain tissues from free DTX- and DTX-NDs-treated healthy mice. The concentration of DTX in the DTX-NDs group was 2.6 and 9 times higher than that in the free DTX group ($p < 0.05$, $n = 4$ for each group), in the non-sonicated and sonicated brains, respectively. Furthermore, the mean ratio of DTX concentration (sonicated relative to non-sonicated brain tissue, Figure 4c) was 4.2 ± 2.6 for DTX-NDs-treated mice and 1.2 ± 0.6 for free DTX-treated mice demonstrating improved brain accumulation of DTX by FUS-BBBD only with the vectorized DTX formulation ($p < 0.05$, $n = 4$ for each group). These findings suggested that i) NDs vectorization of DTX could improve DTX brain availability, and ii) FUS-BBBD could improve DTX brain availability with DTX-NDs formulation only.

Brain Delivery of Docetaxel-Loaded Nanodroplets After Repeated Treatment in Glioma-Bearing Mice

We then investigated whether repeated administration of the DTX-NDs formulation combined with hemispheric FUS-BBBD enhanced DTX accumulation within the brain tumor (see Experimental Design and Treatment Plans of the in vivo Efficacy Studies in Materials and Methods, experimental group 1). Figure 4b illustrates the DTX concentrations per unit mass in sonicated brain tumor tissue and in contralateral healthy brain tissue from free DTX- and DTX-NDs-treated GL261 glioma-bearing mice. The DTX-NDs-treated mice ($n = 3$) displayed a significantly higher concentration of DTX (6-fold higher, $p < 0.05$) than the free DTX-treated mice ($n = 2$), but only in the sonicated tumor sites. The DTX concentration ratio of tumor/contralateral brain is also higher in DTX-NDs-treated mice than in free DTX-treated mice (6.3 ± 5.7 vs. 1.6 ± 0.1, respectively), although not significantly ($p = 0.14$) (Figure 4c). These results suggest that combining the DTX-NDs emulsion with FUS-BBBD and repeating this treatment could increase the cerebral availability of DTX at the tumor site and thus improve its therapeutic efficacy in glioma-bearing mice.

https://doi.org/10.2147/IJN.S571560

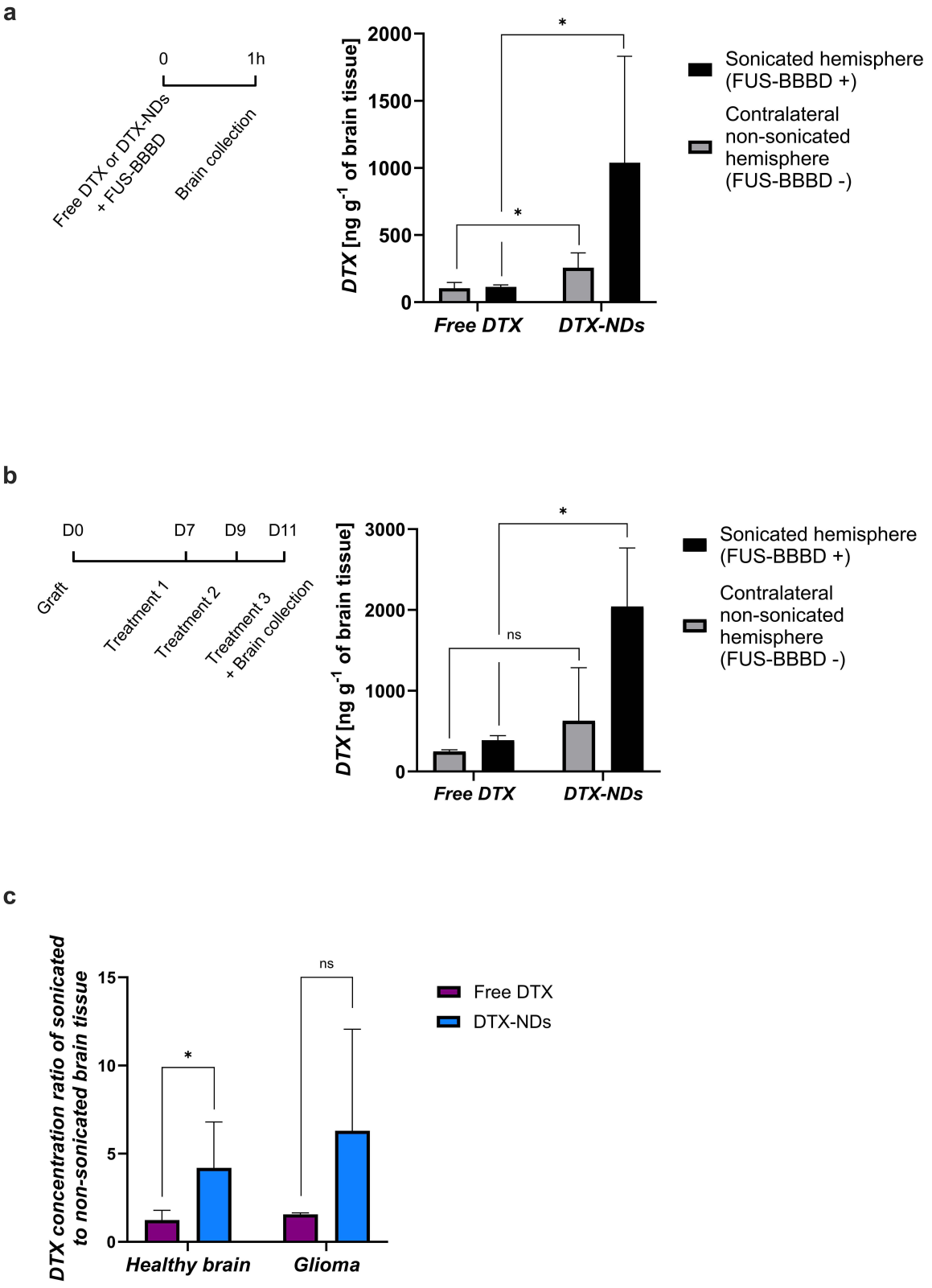

Figure 4 Docetaxel brain accumulation after treatment with free docetaxel (DTX) or docetaxel-loaded nanodroplets formulation (DTX-NDs) in combination with hemispheric FUS-BBBD: (**a**) in healthy mice after a single treatment (free DTX, n = 4 or DTX-NDs, n = 4) or (**b**) in glioma-bearing mice after repeated treatment (free DTX, n = 2 or DTX-NDs, n = 3). (**c**) Docetaxel concentration ratio of sonicated to non-sonicated brain tissue after treatment. FUS-BBBD procedure was performed on the right hemisphere for healthy mice or the hemisphere bearing the tumor for glioma-bearing mice. FUS-BBBD + indicates conditions with hemispheric FUS-BBBD, whereas FUS-BBBD - indicates conditions without hemispheric FUS-BBBD. *p < 0.05, ns: not significant, Student's *t*-test.

https://doi.org/10.2147/IJN.S571560

Therapeutic Efficacy of Docetaxel-Loaded Nanodroplets Delivered by Focused Ultrasound-Mediated Blood-Brain Barrier Disruption in Glioma-Bearing Mice

The GL261 glioma-bearing mice were randomly divided in three groups: control (NaCl 0.9%), free DTX (Docetaxel Accord®) and DTX-NDs. The experimental scheme of treatment over time is shown in Figure 5a and detailed in Experimental Design and Treatment Plans of the in vivo Efficacy Studies in Materials and Methods, experimental group 2 (briefly, 4 administrations combined to FUS-BBBD, equivalent DTX dose of 20 mg kg^{-1}). Animal survival and weight were monitored. Figure 5b shows the Kaplan–Meier survival curves of the three groups and the survival analysis results are summarized in Table 3. The median survival time of mice treated with DTX-NDs (33 days) was significantly prolonged compared to the control group (27 days, $p < 0.01$), representing a 22% IST_{median}. The median survival time of DTX-NDs-treated mice was also longer than that of mice treated with free DTX (20 days), but the difference was not significant. The mean body weight change (% of previous maximum weight) was −4.6 ± 3.3% and −5.4 ± 2.4% ($p = 0.61$) after treatments 1 and 2 (D12), and −12.8 ± 4.6% and −21.1 ± 3.2% ($p < 0.01$) after all four treatments (D20) for the DTX-NDs and free DTX groups, respectively (Figure 5c). These results suggest that repeated administration of DTX-NDs combined with FUS-BBBD is effective in improving survival of glioma-bearing mice. However, the treatment plan is associated with a non-negligible toxicity, even if it is less toxic than free DTX treatment.

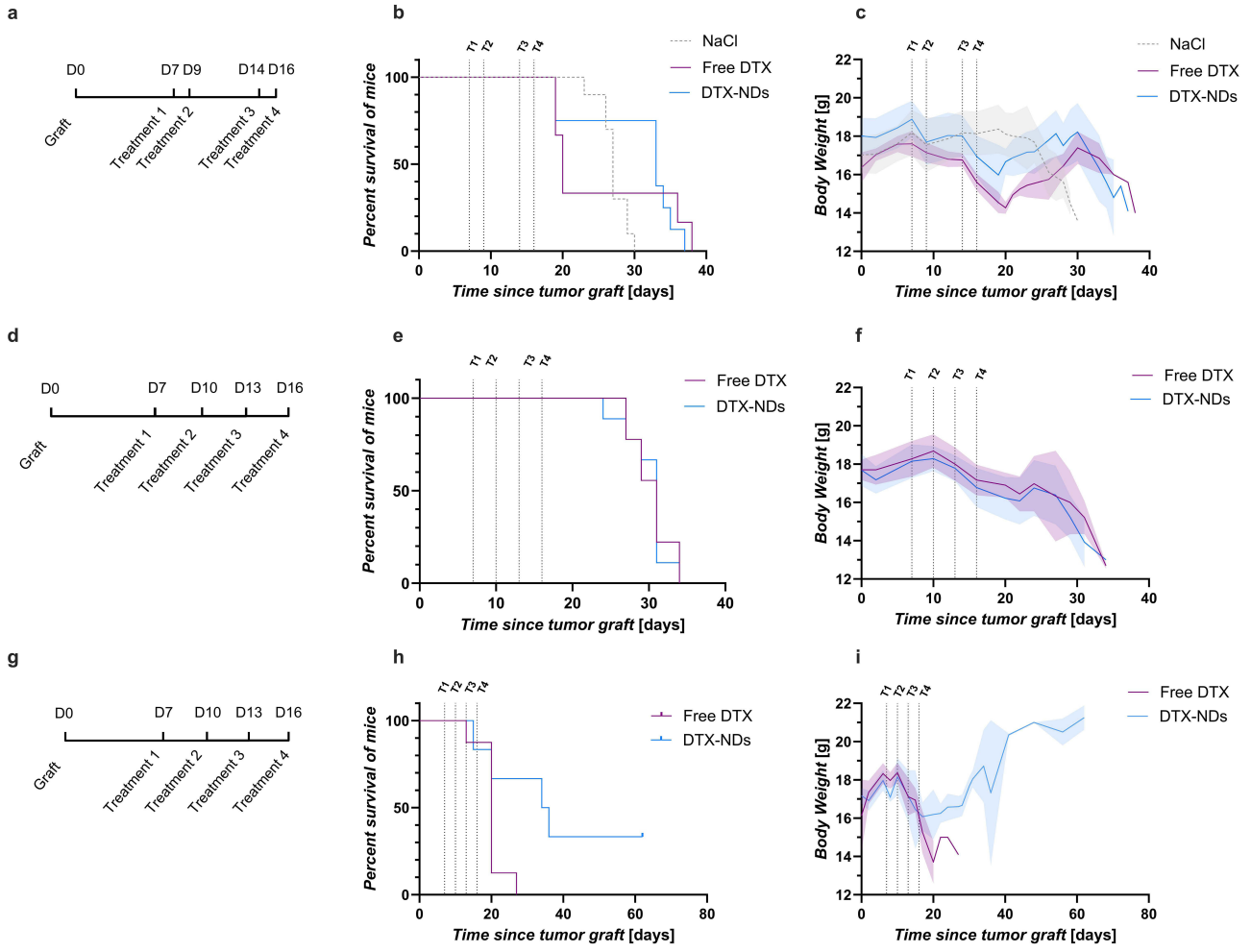

Figure 5 In vivo therapeutic efficacy of DTX-NDs delivered by FUS-BBBD in glioma-bearing mice after adjusted treatment plan. (**a, d** and **g**) In vivo treatment plan of NaCl or free DTX or DTX-NDs combined to FUS-BBBD in glioma-bearing mice according to experimental group 2 (NaCl 0.9%, n = 10, free DTX, n = 6, DTX-NDs, n = 8, equivalent DTX dose of 20 mg kg^{-1}), experimental group 3 (free DTX, n = 9, DTX-NDs = 9, equivalent DTX dose of 20 mg kg^{-1} once, followed by 10 mg kg^{-1}) and experimental group 4 (free DTX, n = 8, DTX-NDs = 6, equivalent DTX dose of 20 mg kg^{-1}). Kaplan-Meier survival curves (**b, e** and **h**) and bodyweight curves (**c, f** and **i**) of glioma-bearing mice in the three experimental groups.

https://doi.org/10.2147/IJN.S571560

Table 3 Survival Analysis According to Various Treatment Plans

	Treatment Group	Maximum Survival [Days]	Median Survival [Days]	IST_{median} vs. Control [%]	P-value	IST_{median} vs. Free DTX [%]	P-value
Experimental group 2	NaCl (control) (n = 10)	30	27	-	-		
	Free DTX (n = 6)	38	20	−26%	0.089	-	-
	DTX-NDs (n = 8)	37	33	+22%	0.008 (**)	+65%	0.834
Experimental group 3	Free DTX (n = 9)	34	31			-	-
	DTX-NDs (n = 9)	34	31			0%	0.878
Experimental group 4	Free DTX (n = 8)	27	20			-	-
	DTX-NDs (n = 6)	62	36			+80%	0.029 (*)

Notes: IST_{median}: Increase in median survival time. * $p < 0.05$, ** $p < 0.01$ Mantel-Cox Log Rank test.

Improvement of Therapeutic Outcomes with Adjusted Treatment Plan

To improve therapeutic outcomes and reduce toxicity (ie, improve the efficacy/tolerability ratio), treatment plan had to be adjusted (Figure 5d and Experimental Design and Treatment Plans of the in vivo Efficacy Studies in Materials and Methods, experimental group 3). The treatment plan was adapted by reducing the dose (eq. 20 mg kg^{-1} of DTX once, followed by eq. 10 mg kg^{-1} for a total of 4 treatments) and extending the interval between administrations to every 72 hours. The median survival time for the DTX-NDs group was similar to that of the free DTX group (31 days) and was shorter than that with the initial treatment plan (Figure 5e and Table 3). No significant difference in mean body weight change was observed after all four treatments (D20) between DTX-NDs and free DTX groups ($p = 0.14$) (Figure 5f). These results may be attributed to a sub-optimal dose of DTX, which was less toxic but not sufficient to achieve a maximal anti-tumor effect.

Therefore, a third treatment plan was tested, that maintained the interval between injections of the second plan (72 hours) but with a maximum dose equivalent to 20 mg kg^{-1} of DTX. Using this protocol (Figure 5g and Experimental Design and Treatment Plans of the in vivo Efficacy Studies in Materials and Methods, experimental group 4), the median survival time of the DTX-NDs group (36 days) was significantly prolonged compared to the free DTX group (20 days, $p < 0.05$), and also to the first treatment plan with DTX-NDs (33 days) (Figure 5b, h and Table 3). Additionally, 2 out of 6 mice treated with DTX-NDs + FUS-BBBD demonstrated long-term survival (> 60 days), whereas none of the mice in the free DTX group survived beyond 27 days (Figure 5h). MRI scans performed during the protocol confirmed that mice with long-term survival in the DTX-NDs group had a tumor (data not shown). Four days after receiving the full treatment plan (D20), the mean weight change was $-12.6 \pm 6.8\%$ and $-26.2 \pm 5.5\%$ ($p < 0.01$) for DTX-NDs group and free DTX group, respectively, requiring over 80% of free DTX-treated mice to be sacrificed at 20 days post-graft of tumor (Figure 5i). Furthermore, we observed an increase in mouse body weight starting 3 days after the last treatment in the DTX-NDs group. Consequently, at equivalent dose of DTX, DTX-NDs emulsion appears to be better tolerated than the branded DTX formulation in combination with FUS-BBBD, while improving glioma-bearing mice survival. Finally, with an optimized treatment plan, the efficacy/tolerability ratio was enhanced solely for the DTX-NDs group.

Discussion

In our previous work, we demonstrated that the F-TAC-stabilized PFOB nanoemulsion exhibits excellent biocompatibility and promising PK behavior. Furthermore, when combined with FUS-BBBD, the intracerebral accumulation of tagged-droplets was significantly and safely enhanced. Taken together, these results highlight the potential of this innovative PFOB nanoemulsion as an effective NC for the cerebral delivery of hydrophobic agents via FUS-BBBD.[19] In the present study, we successfully developed and optimized DTX-NDs for brain tumor delivery, particularly when combined with FUS-BBBD.

DTX, a taxane chemotherapeutic agent, is already approved for the treatment of several solid cancers. DTX can induce glioma cell apoptosis and displays significant inhibitory effects.[29] However, due to its poor water solubility, inability to cross the BBB, and low bioavailability, DTX demonstrates limited brain tumor-targeting efficiency. Various

drug delivery systems have been investigated to improve the tolerability and therapeutic potential of DTX.[30–33] To date, only one micelle-based formulation of DTX has been found in the literature in combination with ultrasound-targeted MB destruction,[34] but none in combination with FUS-BBBD. Here, we propose this approach as a unique opportunity to repurpose a potent anticancer drug for targeted delivery in GBM.

Our DTX-NDs formulation demonstrated properties suitable for systemic delivery, including uniform morphology, controlled size and dispersity (≈ 50–60 nm with Pdi < 0.2), as well as satisfactory DL and EE (> 90%), similar to those of other anticancer drugs-loaded NCs.[17,34,35] Particle size is a critical factor for NC extravasation into the brain parenchyma. The optimal size must be small enough to cross the disrupted tight junctions caused by FUS-BBBD, yet large enough to avoid rapid renal excretion. It is generally accepted that particles should ideally be smaller than 100 nm to ensure brain delivery,[26] with the most efficient delivery achieved using NCs around 50 nm in size.[17] Our NDs are smaller than most drug-loaded NCs previously used with FUS-BBBD (typically around 100 nm or more),[18] except for some inorganic[36,37] and DNA-based nanoparticles.[38] However, organic NCs offer advantages such as biocompatibility, biodegradability, and high DL capacity. In addition, our NDs enable a slow release of DTX (without burst effect), promoting effective drug accumulation in tumor tissue and reducing peripheral toxicity, which is comparable with the cumulative-release profile of DTX-loaded micelles reported by Mao et al[34] Additionally, while reproducibility challenges are often encountered with organic nanoparticles (liposomes and polymers are the main nanomaterials for brain delivery reported in the literature),[11,12] we report a new, reproducible, and freeze-drying-stable DTX-loaded formulation suitable for long-term storage.

In terms of preclinical studies, the PK and the safety profiles of new nanotherapeutics are essential for defining appropriate dosing regimens and ensuring successful clinical translation.[10] Protecting the drug from degradation and prolonging its circulation half-life are key to increasing its accumulation in the brain when the BBB is disrupted. Firstly, the PK profile of our DTX-NDs (reduced blood clearance, reduced tissue distribution, prolonged elimination half-life…) improves the likelihood of BBB crossing (when BBB is disrupted) compared to the commercial formulation. Indeed, our formulation offers sustained DTX release, enhancing drug exposure. Notably, the maximum BBB permeability achieved with our protocol reaches approximately 65 nm,[26,27] which is consistent with the size of our DTX-NDs. Secondly, no major irreversible organ toxicity was observed with our formulation. Transient hepatotoxicity was in line with our previous observations,[19] which showed a temporary liver accumulation of PFOB, reduced by half within 48 hours and completely resolved by 72 hours. Besides that, there were no signs of renal suffering or inflammation. Overall, the PK and safety profiles of DTX-NDs (complete excretion in 8.4 hours (ie, 7 $t_{1/2}$), transient hepatic accumulation) support the feasibility and safety of repeated administration. This is particularly important since repeated FUS-BBBD sessions are likely required for effective GBM treatment. Although this study provides a detailed, time-resolved PK profile based on dense sampling (nine time points, n = 5 per time point), formal population pharmacokinetic modeling was not feasible due to the inability to perform repeated blood sampling in the same mice. Future studies could address population-based analyses using appropriate animal models to improve translational relevance.

In addition to demonstrating reduced peripheral toxicity, our results show that DTX-NDs enhance brain availability of DTX, and that FUS-BBBD can further improve DTX availability in the brain and tumor when formulated into droplets. DTX is a substrate of P-glycoprotein (P-gp),[39] a major efflux transporter at the BBB. While sonication can locally reduce P-gp expression and potentially enhance the intracerebral substrate accumulation,[40,41] Goutal et al found that such modulation may be insufficient alone.[42,43] This could explain the weak enhancement of DTX concentration in the brain and the lack of therapeutic benefit observed with free DTX when combined with FUS-BBBD. In addition, the surfactants constituting the shell of DTX-NDs may inhibit P-gp activity,[44] which could partially account for the improved DTX intracerebral retention observed with the NDs formulation even without FUS-BBBD. Literature reports an average 6.2-fold increase in drug accumulation in brain tumors after FUS-BBBD with nanoparticle-based drug conjugates, which is consistent with our results (4.2 ± 2.6 in healthy mice and 6.3 ± 5.7 in tumor-bearing mice).[17]

Furthermore, although DTX-NDs significantly enhance DTX brain accumulation by 2.6-fold without FUS-BBBD, the relatively low accumulation levels likely preclude therapeutic efficacy. Moreover, our previous findings confirmed limited passive diffusion of our dye-loaded NDs, as no fluorescence was detected in the intact BBB hemisphere.[19] Therefore, only the combination of DTX-NDs and FUS-BBBD was tested, and compared to the combination of free DTX and FUS-BBBD. Evaluating the benefits of drug vectorization by comparing vectorized drug to free drug remains crucial, yet is poorly studied

in most preclinical studies investigating drug-loaded NCs in association with FUS-BBBD.[18] We demonstrated that repeated administration of DTX-NDs formulation combined with FUS-BBBD improved animal survival, with adaptation of the protocol, without inducing significant toxicity in mice. The treatment plan was optimized to balance efficacy and tolerability. The initial protocol (20 mg kg^{-1} of DTX, 2 sessions of 2 administrations 48 hours apart) was selected on the basis of PK and safety results. This dose of 20 mg kg^{-1} of DTX (the highest dose found in the literature) provides superior therapeutic efficacy compared to doses of 5 or 10 mg kg^{-1} using a DTX-loaded nanoemulsion in a murine brain tumor model.[29] In our study, this protocol significantly increased the survival of mice treated with DTX-NDs emulsion by 22% as compared to the control group (median survival 33 vs. 27 days, $p < 0.05$) and an improvement by 65% as compared to free DTX-treated mice, though this was not significant. Higher toxicity with free DTX was expected, as it led to significantly greater body weight loss than vectorized DTX in several murine models.[22,29,45] The toxicity observed in mice treated with free DTX likely explains their poor median survival (20 days). Reducing the dose to 10 mg kg^{-1}, except for the first administration kept at 20 mg kg^{-1}, and extending the dosing interval to 72 hours improved the tolerability in free DTX-treated mice, but eliminated the difference in efficacy between the DTX-NDs and the free DTX groups, probably due to the loss of efficacy in DTX-NDs-treated group. The optimal treatment plan was then determined (20 mg kg^{-1} of DTX, every 72 hours, total of 4 sessions). This resulted in an improved efficacy/tolerability ratio for the DTX-NDs formulation, with an IST_{median} of 80%, a significantly enhanced tolerability compared to free DTX, and two long-surviving animals (33% of animals).

In this study, we developed a new formulation of DTX that, when combined with FUS-BBBD, improves survival in GBM-bearing mice. One limitation of our work could be the absence of a clear link between in vitro and in vivo efficacy and the lack of a dose–response assessment for DTX. Since our NDs are biocompatible[19] and DTX activity is preserved, no in vitro differences were expected in 2D cultures. Moreover, 3D spheroids are not suitable, as the oil phase promoted adherent cell proliferation (data not shown).

This work also paves the way for several perspectives. First, the therapeutic regimen strongly influences the benefit-risk balance. Pilot studies and Pharmacokinetic/Pharmacodynamic modeling could optimize protocols and enhance cerebral accumulation.[46] Second, as maximal safe resection remains standard for GBM, DTX-NDs should be tested in models including surgery to assess their ability to prevent recurrence.[47,48] Finally, multimodal strategies may further improve brain or tumor penetration, such as combining active targeting or a "Trojan horse" approach with FUS-BBBD.[11] Controlled release from NDs during the BBB permeability window could also increase DTX accumulation. The integration of targeting with on-demand release may provide synergistic therapeutic efficacy.

Conclusion

In summary, we developed a novel strategy combining DTX-loaded perfluorocarbon NDs with FUS-BBBD for the treatment of GBM. This biocompatible delivery system is suitable for repeated administrations, and offers enhanced brain drug delivery while minimizing peripheral toxicity, thereby improving therapeutic efficacy. Future studies will focus on optimizing therapeutic regimens through Pharmacokinetic/Pharmacodynamic modeling, evaluating efficacy in clinically relevant models including post-surgical settings, and exploring multimodal strategies such as targeted delivery and controlled release to further improve brain and tumor penetration. Together, these perspectives highlight the translational potential of this approach for improving prognosis of GBM patients.

Abbreviations

ACN, acetonitrile; ALAT, alanine aminotransferase; ASAT, Aspartate aminotransferase; ATBC, tributyl O-acetyl citrate; AUC, area under the curve; BBB, blood–brain barrier; BTB, blood-tumor barrier; C-90, Capryol® 90; Cl, total clearance; C_{max}, concentration at the 5th minute after the end of i.v. injection; D_H, Hydrodynamic diameter; DL, Drug loading; DLS, Dynamic Light Scattering; DMEM, Dulbecco's Modified Eagle Medium; DPBS, Dulbecco's Phosphate-Buffered Saline; DTX, docetaxel; DTX-NDs, Docetaxel-loaded nanodroplets; EE, encapsulation efficiency; FCS, fetal calf serum; F-TAC, fluorinated surfactant; FUS-BBBD, focused ultrasound-mediated blood–brain barrier disruption; Fv, volume fraction; GBM, glioblastoma; HPLC, high performance liquid chromatography; IL-6, interleukin-6; IS, internal standard; IST_{median}, increase in median survival time; LC-MS, liquid chromatography-mass spectrometry; MBs, microbubbles;

MRI, magnetic resonance imaging; MTBE, methyl tert-butyl ether; MTT, 3-(4,5-dimethylthiazol-2-yl)-2,5-diphenyltetrazolium bromide; NCs, nanocarriers; NDs, nanodroplets; PBS, Phosphate Buffer Saline; Pdi, polydispersity index; PFOB, perfluorooctyl bromide; P-gp, P-glycoprotein; PK, pharmacokinetic; PTX, paclitaxel; PTX-NDs, paclitaxel-loaded nanodroplets; Sur, concentration of surfactant; TEM, transmission electron microscopy; $t_{1/2}$, terminal half-life; ULN, upper limit of normal; V_d, volume of distribution.

Data Sharing Statement

The data that support the findings of this study are available from the corresponding authors upon reasonable request. Data related to the synthesis and characterization of the nanoformulation will be available from Dr. Contino-Pépin, while data related to the biological application and animal studies will be available from Dr. Estève.

Ethics Approval

The animal study protocol was approved by Regional Ethics Committee of Aix Marseille Université (protocol code CE71) and authorized by the Directorate General for Research and Innovation (project reference: APAFIS#26725-2020052816206649, approval date: August 28, 2020, and laboratory accreditation number: A1305532).

Acknowledgments

The authors thank I. Bornard (INRAE, Avignon) for TEM acquisitions.

Author Contributions

All authors made a significant contribution to the work reported, whether that is in the conception, study design, execution, acquisition of data, analysis and interpretation, or in all these areas; took part in drafting, revising or critically reviewing the article; gave final approval of the version to be published; have agreed on the journal to which the article has been submitted; and agree to be accountable for all aspects of the work.

Funding

This research was funded with financial support from ITMO Cancer AVIESAN (Alliance Nationale pour les Sciences de la Vie et de la Santé, National Alliance for Life Sciences & Health) within the framework of the Cancer Plan; from European Regional Development Fund; from French Government; from the Sud Provence-Alpes-Côte d'Azur Region; from the Departmental Council of Vaucluse and the Urban Community of Avignon.

Disclosure

Dr Anthony Novell and Dr Benoit Larrat are co-founders of TheraSonic, a company developing a medical device for ultrasound-induced blood–brain barrier opening in patients. Dr Benoit Larrat reports personal fees from TheraSonic, outside the submitted work. The authors report no other conflicts of interest in this work.

References

1. Ostrom QT, Gittleman H, Truitt G, Boscia A, Kruchko C, Barnholtz-Sloan JS. CBTRUS statistical report: primary brain and other central nervous system tumors diagnosed in the United States in 2011–2015. *Neuro-Oncology*. 2018;20(suppl_4):iv1–iv86. doi:10.1093/neuonc/noy131
2. Stupp R, Taillibert S, Kanner A, et al. Effect of tumor-treating fields plus maintenance temozolomide vs maintenance temozolomide alone on survival in patients with glioblastoma: a randomized clinical trial. *JAMA*. 2017;318(23):2306–2316. doi:10.1001/jama.2017.18718
3. Tan AC, Ashley DM, López GY, Malinzak M, Friedman HS, Khasraw M. Management of glioblastoma: state of the art and future directions. *Ca A Cancer J Clinicians*. 2020;70(4):299–312. doi:10.3322/caac.21613
4. Stupp R, Mason WP, Van Den Bent MJ, et al. Radiotherapy plus concomitant and adjuvant temozolomide for glioblastoma. *N Engl J Med*. 2005;352(10):987–996. doi:10.1056/NEJMoa043330
5. Tykocki T, Eltayeb M. Ten-year survival in glioblastoma. A systematic review. *J Clin Neurosci*. 2018;54:7–13. doi:10.1016/j.jocn.2018.05.002
6. Arvanitis CD, Ferraro GB, Jain RK. The blood–brain barrier and blood–tumour barrier in brain tumours and metastases. *Nat Rev Cancer*. 2020;20(1):26–41. doi:10.1038/s41568-019-0205-x
7. Sarkaria JN, Hu LS, Parney IF, et al. Is the blood–brain barrier really disrupted in all glioblastomas? A critical assessment of existing clinical data. *Neuro-Oncology*. 2018;20(2):184–191. doi:10.1093/neuonc/nox175

8. Van Tellingen O, Yetkin-Arik B, De Gooijer MC, Wesseling P, Wurdinger T, De Vries HE. Overcoming the blood–brain tumor barrier for effective glioblastoma treatment. *Drug Resist Updates*. 2015;19:1–12. doi:10.1016/j.drup.2015.02.002
9. Terstappen GC, Meyer AH, Bell RD, Zhang W. Strategies for delivering therapeutics across the blood-brain barrier. *Nat Rev Drug Discov*. 2021;20 (5):362–383. doi:10.1038/s41573-021-00139-y
10. Pedder JH, Sonabend AM, Cearns MD, et al. Crossing the blood-brain barrier: emerging therapeutic strategies for neurological disease. *Lancet Neurol*. 2025;24(3):246–260. doi:10.1016/S1474-4422(24)00476-9
11. Lim SH, Yee GT, Khang D. Nanoparticle-Based combinational strategies for overcoming the blood-brain barrier and blood-tumor barrier. *Int J Nanomed*. 2024;19:2529–2552. doi:10.2147/IJN.S450853
12. Tsou YH, Zhang XQ, Zhu H, Syed S, Xu X. Drug delivery to the brain across the blood–brain barrier using nanomaterials. *Small*. 2017;13(43). doi:10.1002/smll.201701921
13. Meng Y, Pople CB, Lea-Banks H, et al. Safety and efficacy of focused ultrasound induced blood-brain barrier opening, an integrative review of animal and human studies. *J Control Release*. 2019;309:25–36. doi:10.1016/j.jconrel.2019.07.023
14. Horodyckid C, Canney M, Vignot A, et al. Safe long-term repeated disruption of the blood-brain barrier using an implantable ultrasound device: a multiparametric study in a primate model. *J Neurosurg*. 2017;126(4):1351–1361. doi:10.3171/2016.3.JNS151635
15. Olumolade OO, Wang S, Samiotaki G, Konofagou EE. Longitudinal motor and behavioral assessment of blood–brain barrier opening with transcranial focused ultrasound. *Ultrasound Med Biol*. 2016;42(9):2270–2282. doi:10.1016/j.ultrasmedbio.2016.05.004
16. Beccaria K, Canney M, Bouchoux G, et al. Ultrasound-induced blood-brain barrier disruption for the treatment of gliomas and other primary CNS tumors. *Cancer Lett*. 2020;479:13–22. doi:10.1016/j.canlet.2020.02.013
17. Schoen S, Kilinc MS, Lee H, et al. Towards controlled drug delivery in brain tumors with microbubble-enhanced focused ultrasound. *Adv Drug Deliv Rev*. 2022;180:114043. doi:10.1016/j.addr.2021.114043
18. Bérard C, Truillet C, Larrat B, et al. Anticancer drug delivery by focused ultrasound-mediated blood-brain/tumor barrier disruption for glioma therapy: from benchside to bedside. *Pharmacol Ther*. 2023;250:108518. doi:10.1016/j.pharmthera.2023.108518
19. Bérard C, Desgranges S, Dumas N, et al. Perfluorocarbon nanodroplets as potential nanocarriers for brain delivery assisted by focused ultrasound-mediated blood-brain barrier disruption. *Pharmaceutics*. 2022;14(7):1498. doi:10.3390/pharmaceutics14071498
20. Fan R, Chuan D, Hou H, et al. Development of a hybrid nanocarrier-recognizing tumor vasculature and penetrating the BBB for glioblastoma multi-targeting therapy. *Nanoscale*. 2019;11(23):11285–11304. doi:10.1039/C9NR01320B
21. Kadiyala P, Li D, Nuñez FM, et al. High-density lipoprotein-mimicking nanodiscs for chemo-immunotherapy against glioblastoma multiforme. *ACS Nano*. 2019:acsnano.8b06842. 10.1021/acsnano.8b06842.
22. Kadari A, Pooja D, Gora RH, et al. Design of multifunctional peptide collaborated and docetaxel loaded lipid nanoparticles for antiglioma therapy. *Eur J Pharm Biopharm*. 2018;132:168–179. doi:10.1016/j.ejpb.2018.09.012
23. Correard F, Maximova K, Estève MA, et al. Gold nanoparticles prepared by laser ablation in aqueous biocompatible solutions: assessment of safety and biological identity for nanomedicine applications. *Int J Nanomed*. 2014;9:5415–5430. doi:10.2147/IJN.S65817
24. Felix MS, Borloz E, Metwally K, et al. Ultrasound-Mediated blood-brain barrier opening improves whole brain gene delivery in mice. *Pharmaceutics*. 2021;13(8):1245. doi:10.3390/pharmaceutics13081245
25. Yin YM, Cui FD, Mu CF, et al. Docetaxel microemulsion for enhanced oral bioavailability: preparation and in vitro and in vivo evaluation. *J Control Release*. 2009;140(2):86–94. doi:10.1016/j.jconrel.2009.08.015
26. Marty B, Larrat B, Van Landeghem M, et al. Dynamic study of blood–brain barrier closure after its disruption using ultrasound: a quantitative analysis. *J Cereb Blood Flow Metab*. 2012;32(10):1948–1958. doi:10.1038/jcbfm.2012.100
27. Conti A, Mériaux S, Larrat B. About the Marty model of blood-brain barrier closure after its disruption using focused ultrasound. *Phys Med Biol*. 2019;64(14):14NT02. doi:10.1088/1361-6560/ab259d
28. Stahl FR, Jung R, Jazbutyte V, et al. Laboratory diagnostics of murine blood for detection of mouse cytomegalovirus (MCMV)-induced hepatitis. *Sci Rep*. 2018;8(1):14823. doi:10.1038/s41598-018-33167-7
29. Gaoe H, Pang Z, Pan S, et al. Anti-glioma effect and safety of docetaxel-loaded nanoemulsion. *Arch Pharm Res*. 2012;35(2):333–341. doi:10.1007/s12272-012-0214-8
30. Di Filippo LD, Lobato Duarte J, Hofstätter Azambuja J, et al. Glioblastoma multiforme targeted delivery of docetaxel using bevacizumab-modified nanostructured lipid carriers impair in vitro cell growth and in vivo tumor progression. *Int J Pharm*. 2022;618:121682. doi:10.1016/j.ijpharm.2022.121682
31. Qi N, Zhang S, Zhou X, et al. Combined integrin αvβ3 and lactoferrin receptor targeted docetaxel liposomes enhance the brain targeting effect and anti-glioma effect. *J Nanobiotechnol*. 2021;19(1):446. doi:10.1186/s12951-021-01180-0
32. Luiz MT, Viegas JSR, Abriata JP, et al. Docetaxel-loaded folate-modified TPGS-transfersomes for glioblastoma multiforme treatment. *Mater Sci Eng C Mater Biol Appl*. 2021;124:112033. doi:10.1016/j.msec.2021.112033
33. Ding Y, Xu Q, Chai Z, et al. All-stage targeted red blood cell membrane-coated docetaxel nanocrystals for glioma treatment. *J Control Release*. 2024;369:325–334. doi:10.1016/j.jconrel.2024.03.055
34. Mao K, Jiang Q, Jiang Y, et al. Ultra-small micelles together with UTMD enhanced the therapeutic effect of docetaxel on Glioblastoma. *Eur J Pharm Sci*. 2023;187:106468. doi:10.1016/j.ejps.2023.106468
35. Timbie KF, Afzal U, Date A, et al. MR image-guided delivery of cisplatin-loaded brain-penetrating nanoparticles to invasive glioma with focused ultrasound. *J Control Release*. 2017;263:120–131. doi:10.1016/j.jconrel.2017.03.017
36. Coluccia D, Figueiredo CA, Wu MY, et al. Enhancing glioblastoma treatment using cisplatin-gold-nanoparticle conjugates and targeted delivery with magnetic resonance-guided focused ultrasound. *Nanomed Nanotechnol Biol Med*. 2018;14(4):1137–1148. doi:10.1016/j.nano.2018.01.021
37. Wu M, Chen W, Chen Y, et al. Focused ultrasound-augmented delivery of biodegradable multifunctional nanoplatforms for imaging-guided brain tumor treatment. *Adv Sci*. 2018;5(4):1700474. doi:10.1002/advs.201700474
38. Shen Y, Hu M, Li W, et al. Delivery of DNA octahedra enhanced by focused ultrasound with microbubbles for glioma therapy. *J Control Release*. 2022;350:158–174. doi:10.1016/j.jconrel.2022.08.019
39. Shirakawa K, Takara K, Tanigawara Y, et al. Interaction of docetaxel ("Taxotere") with human P-glycoprotein. *Jpn J Cancer Res*. 1999;90 (12):1380–1386. doi:10.1111/j.1349-7006.1999.tb00723.x

40. Aryal M, Fischer K, Gentile C, Gitto S, Zhang YZ, McDannold N. Effects on P-Glycoprotein expression after blood-brain barrier disruption using focused ultrasound and microbubbles. *PLoS One*. 2017;12(1):e0166061. doi:10.1371/journal.pone.0166061
41. Cho H, Lee HY, Han M, et al. Localized down-regulation of P-glycoprotein by focused ultrasound and microbubbles induced blood-brain barrier disruption in rat brain. *Sci Rep*. 2016;6(1):31201. doi:10.1038/srep31201
42. Goutal S, Gerstenmayer M, Auvity S, et al. Physical blood-brain barrier disruption induced by focused ultrasound does not overcome the transporter-mediated efflux of erlotinib. *J Control Release*. 2018;292:210–220. doi:10.1016/j.jconrel.2018.11.009
43. Goutal S, Novell A, Leterrier S, et al. Imaging the impact of blood-brain barrier disruption induced by focused ultrasound on P-glycoprotein function. *J Control Release*. 2023;361:483–492. doi:10.1016/j.jconrel.2023.08.012
44. Ferraris C, Cavalli R, Panciani PP, Battaglia L. Overcoming the blood–brain barrier: successes and challenges in developing nanoparticle-mediated drug delivery systems for the treatment of brain tumours. *Int J Nanomed*. 2020;15:2999–3022. doi:10.2147/IJN.S231479
45. Kim H, Lee Y, Lee IH, et al. Synthesis and therapeutic evaluation of an aptide-docetaxel conjugate targeting tumor-associated fibronectin. *J Control Release*. 2014;178:118–124. doi:10.1016/j.jconrel.2014.01.015
46. Arvanitis CD, Askoxylakis V, Guo Y, et al. Mechanisms of enhanced drug delivery in brain metastases with focused ultrasound-induced blood-tumor barrier disruption. *Proc Natl Acad Sci U S A*. 2018;115(37):E8717–E8726. doi:10.1073/pnas.1807105115
47. Bastiancich C, Lemaire L, Bianco J, et al. Evaluation of lauroyl-gemcitabine-loaded hydrogel efficacy in glioblastoma rat models. *Nanomedicine*. 2018;13(16):1999–2013. doi:10.2217/nnm-2018-0057
48. Bastiancich C, Snacel-Fazy E, Fernandez S, et al. Tailoring glioblastoma treatment based on longitudinal analysis of post-surgical tumor microenvironment. *J Exp Clin Cancer Res*. 2024;43(1):311. doi:10.1186/s13046-024-03231-4